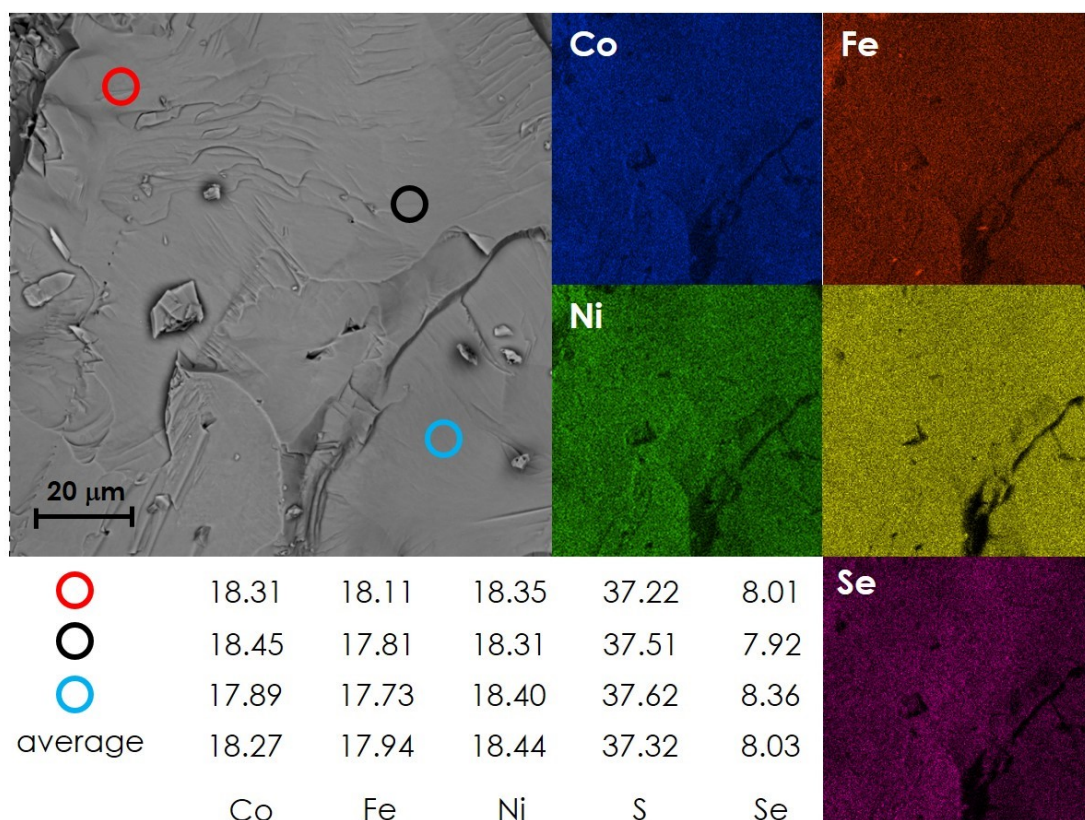
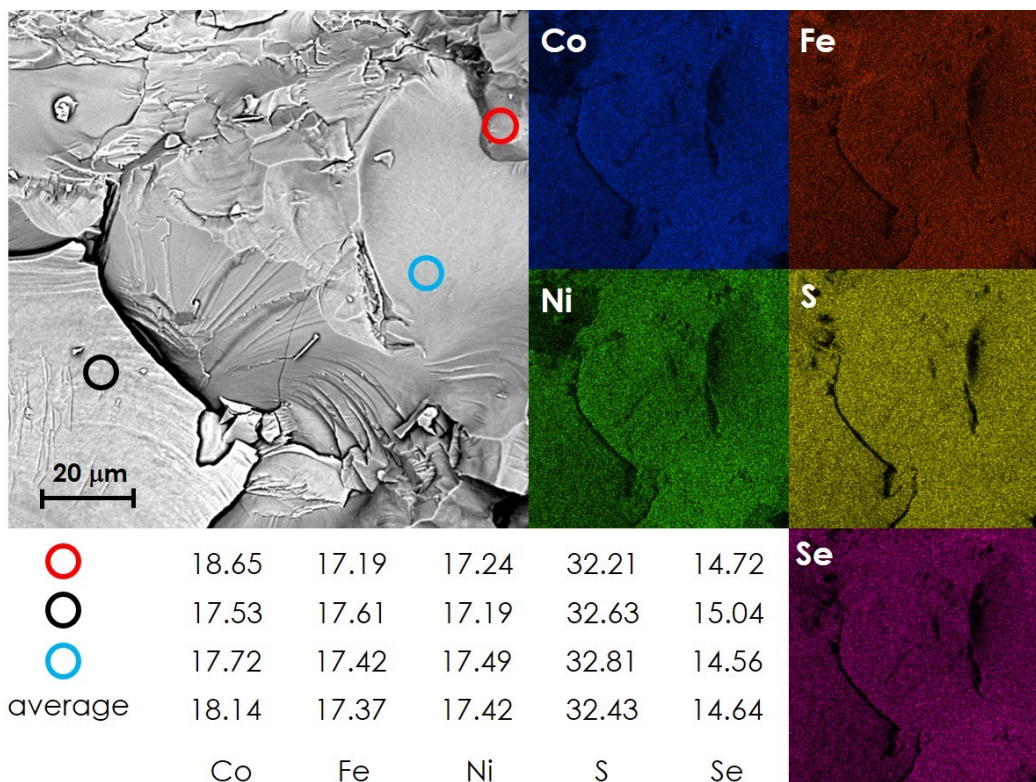


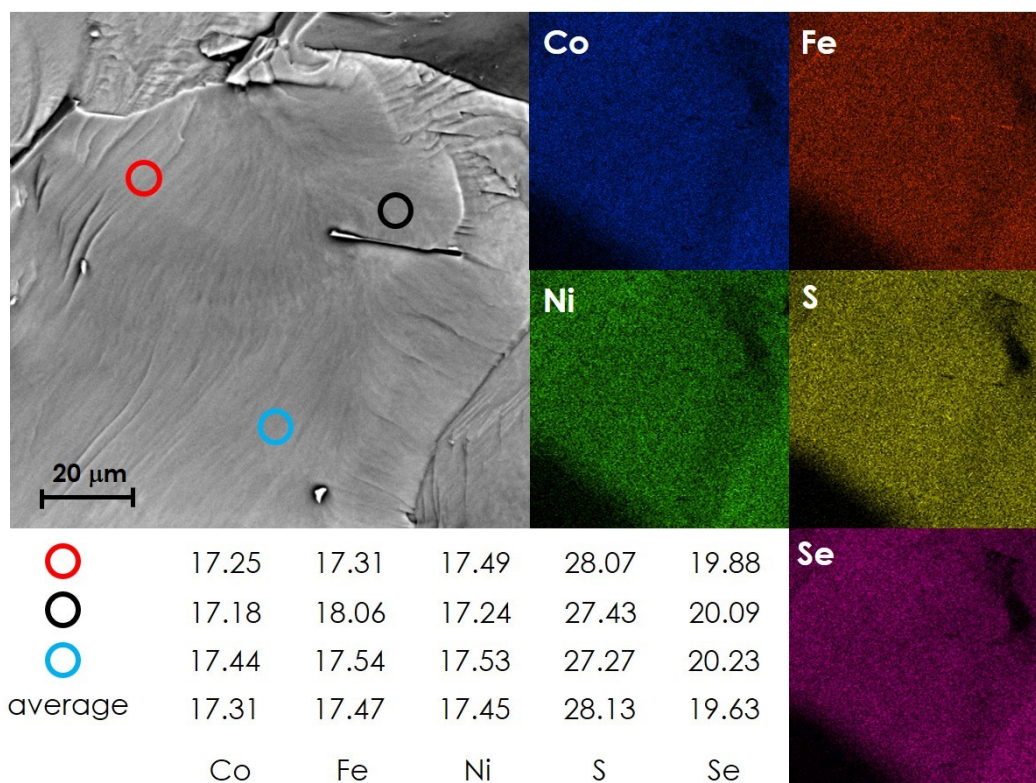
SI Fig. 1 Cross-sectional SEM micrograph together with EDS point and map analysis (at. %) of the  $TM_9S_8$  sample.



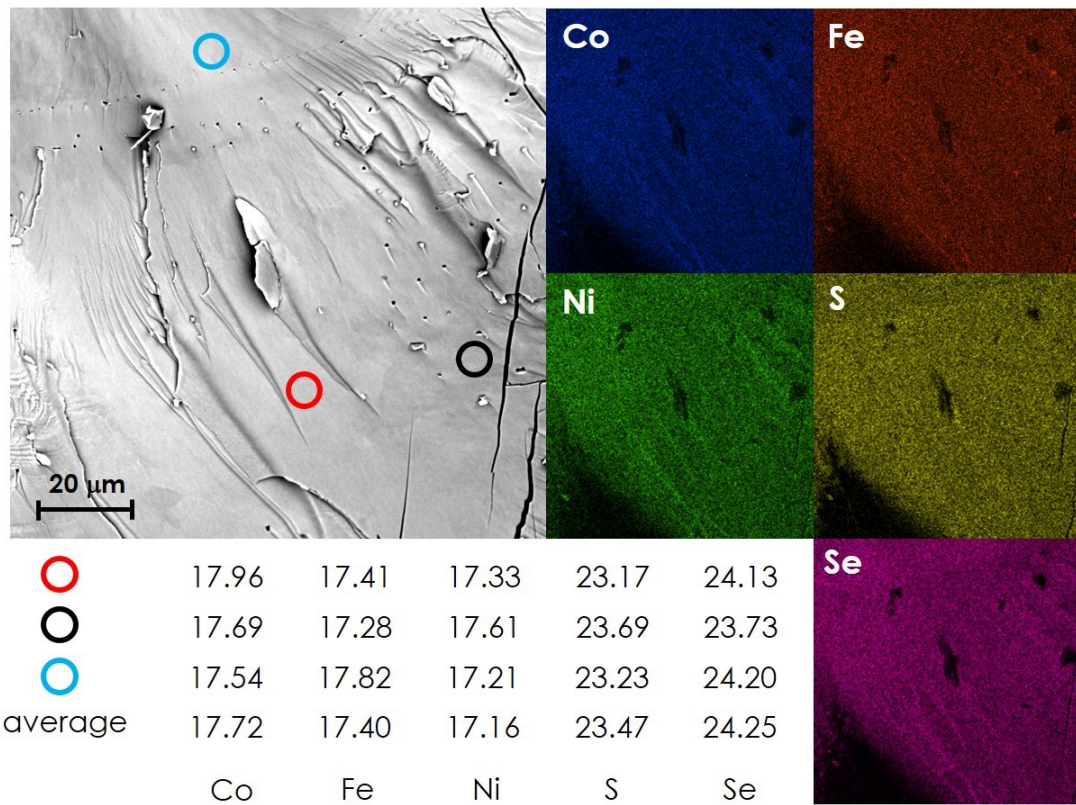
SI Fig. 2 Cross-sectional SEM micrograph together with EDS point and map analysis (at. %) for  $TM_9S_7Se$  sample.



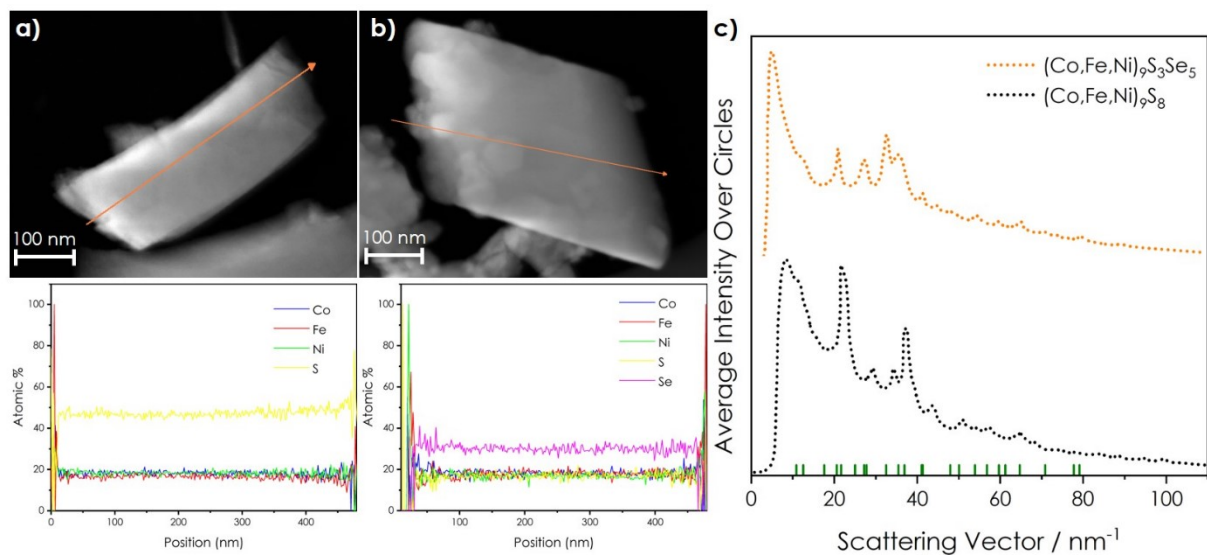
SI Fig. 3 Cross-sectional SEM micrograph together with EDS point and map analysis (at. %) for  $TM_9S_6Se_2$  sample.



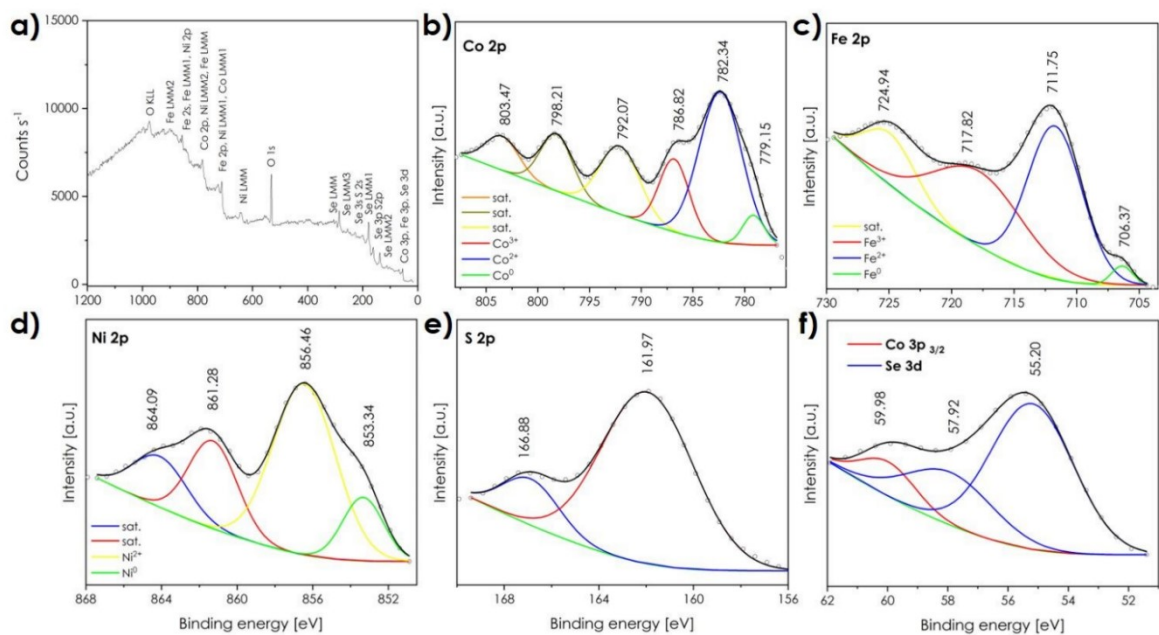
SI Fig. 4 Cross-sectional SEM micrograph together with EDS point and map analysis (at. %) for  $TM_9S_5Se_3$  sample.



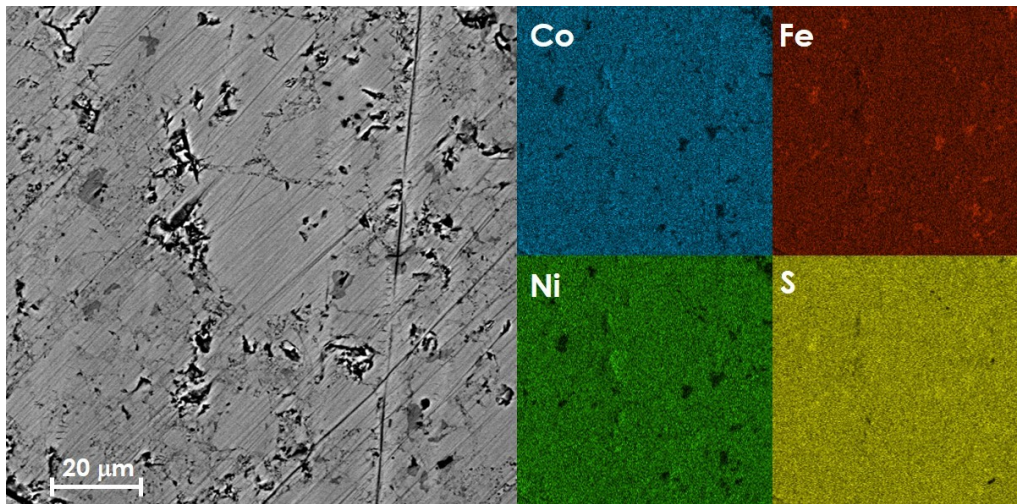
SI Fig. 5 Cross-sectional SEM micrograph together with EDS point and map analysis (at. %) for  $TM_6S_2Se_4$  sample.



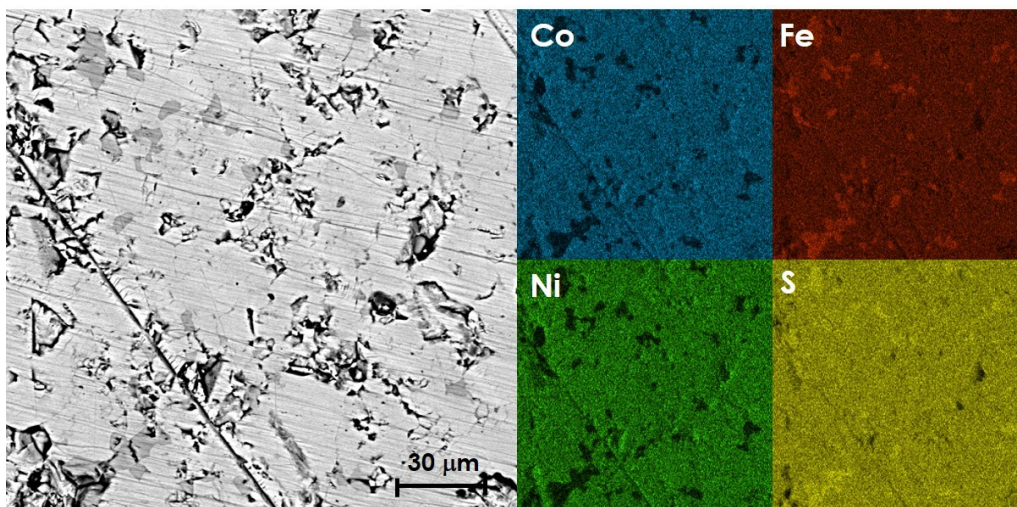
SI Fig. 6 Transmission electron microscopy results: micrographs together with EDS line-scan across the grains for  $\text{TM}_9\text{S}_8$  (a) and  $\text{TM}_9\text{S}_3\text{Se}_5$  (b) sample; intensity of electron diffraction versus scattering vector obtained by circular integration of SAED patterns (c).



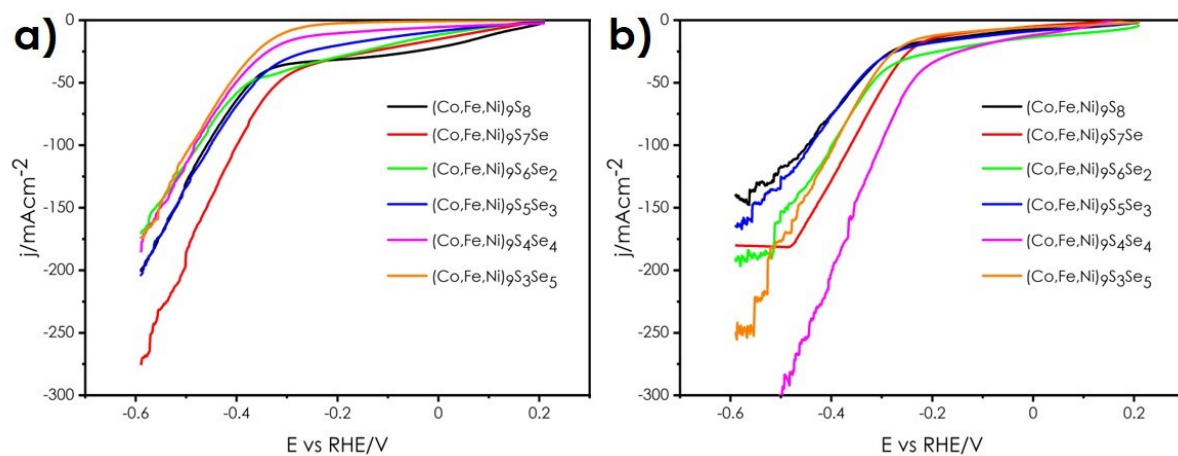
SI Fig. 7 XPS data of  $Co_3Fe_3Ni_3S_4Se_4$  pentlandite: a) XPS survey spectrum, b) Co 2p, c) Fe 2p, d) Ni 2p, e) S 2p, and f) combined Co 3p and Se 3d deconvoluted core level spectra.



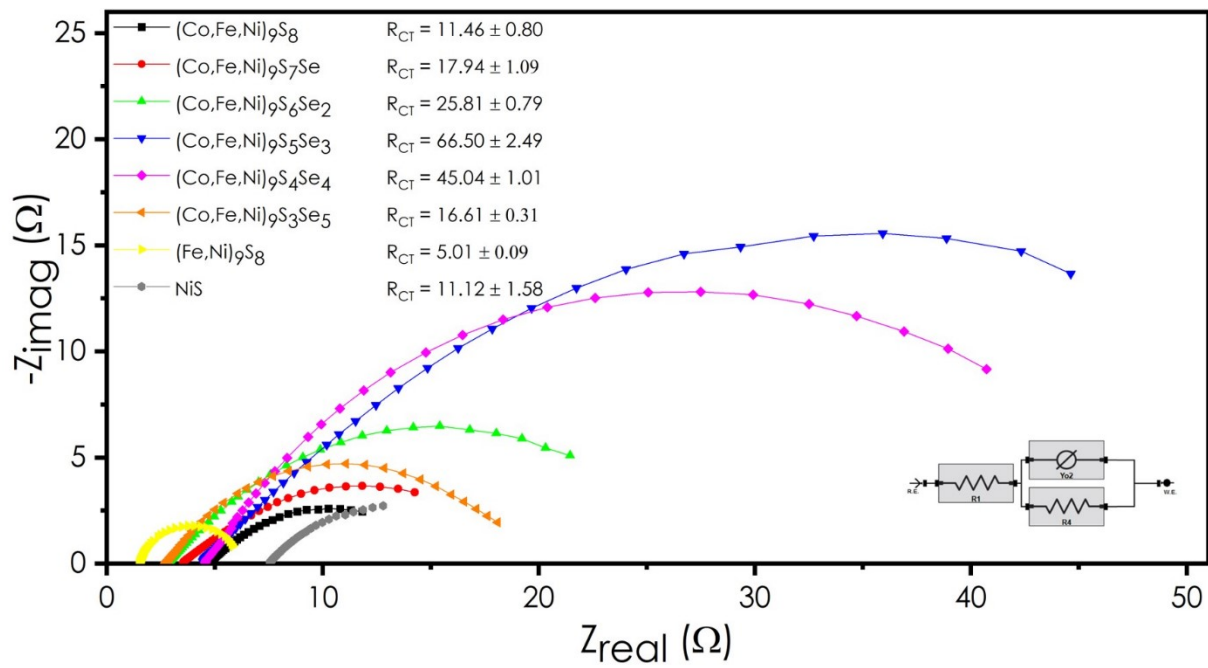
SI Fig. 8 SEM micrograph together with EDS map analysis for  $TM_9S_8$  sample sintered at 450 °C. Averaged sulfur content equal to 43.2 mol. %



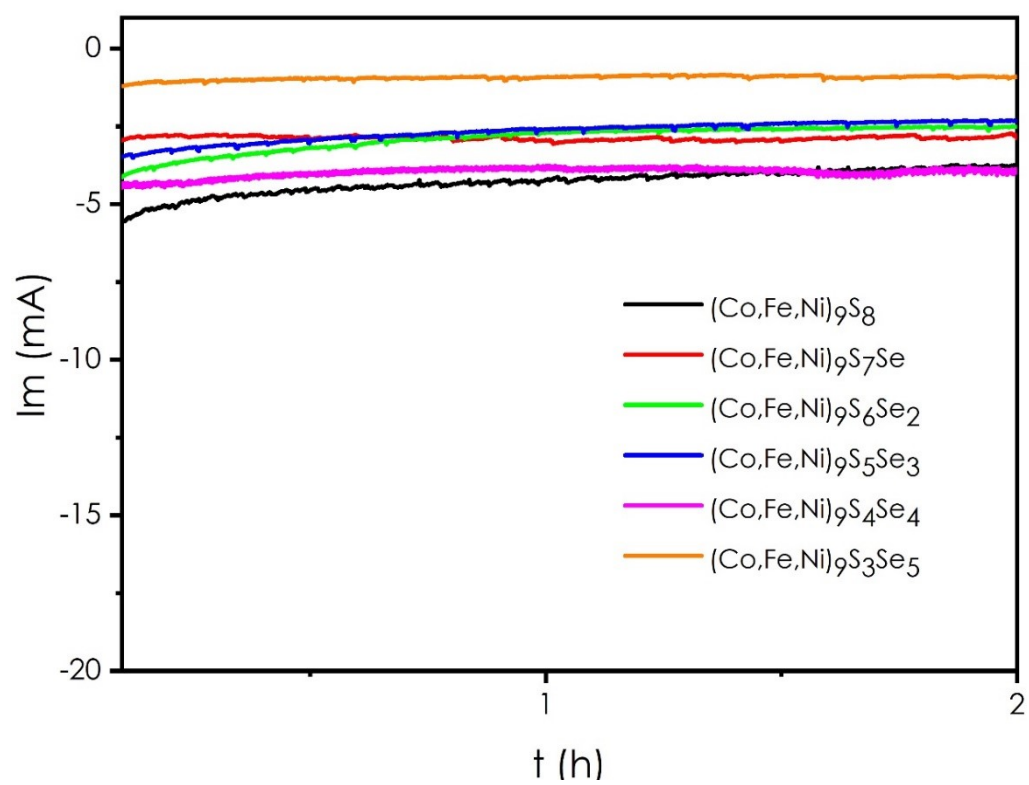
SI Fig. 9 SEM micrograph together with EDS map analysis for  $TM_9S_8$  sample sintered at 500 °C. Averaged sulfur content equal to 40.8 mol. %



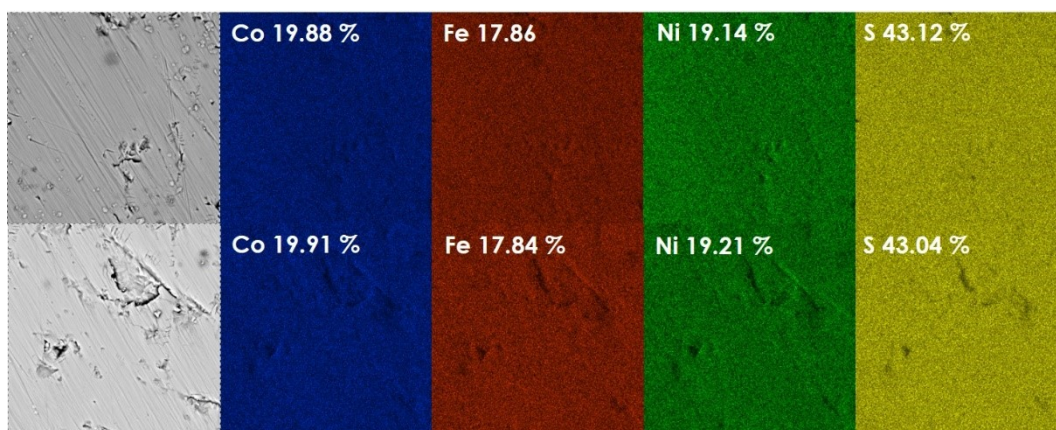
SI Fig. 10 LSV curves as a function of Se concentration normalized to geometric area recorded at sweep rate  $6.25 \text{ mV s}^{-1}$  at  $0.5 \text{ M H}_2\text{SO}_4$ :  
 a) pellets with random particle sizes, b) pellets with normalized particle sizes.



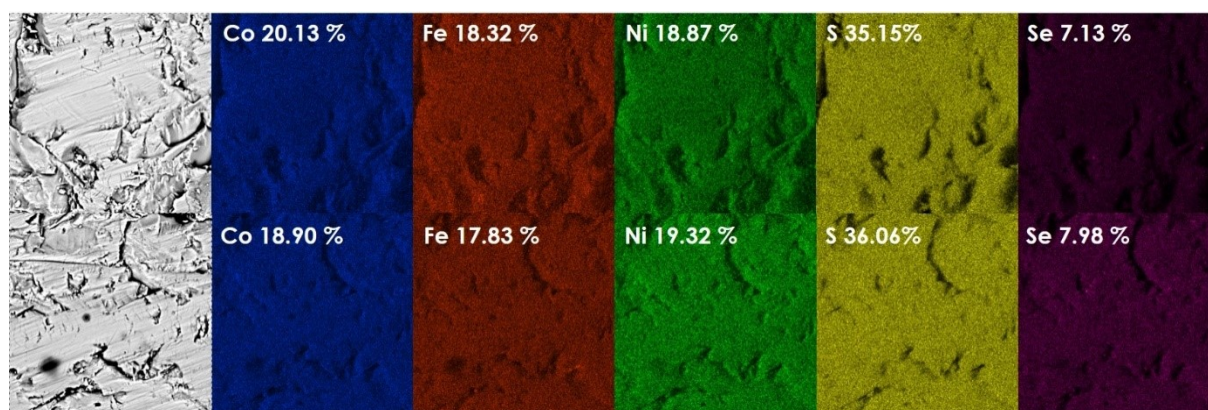
SI Fig.11 Impedance measurements: Nyquist plot of the  $Co_3Fe_3Ni_3S_{8-x}Se_x$  normalized series together with calculated charge transfer resistance.



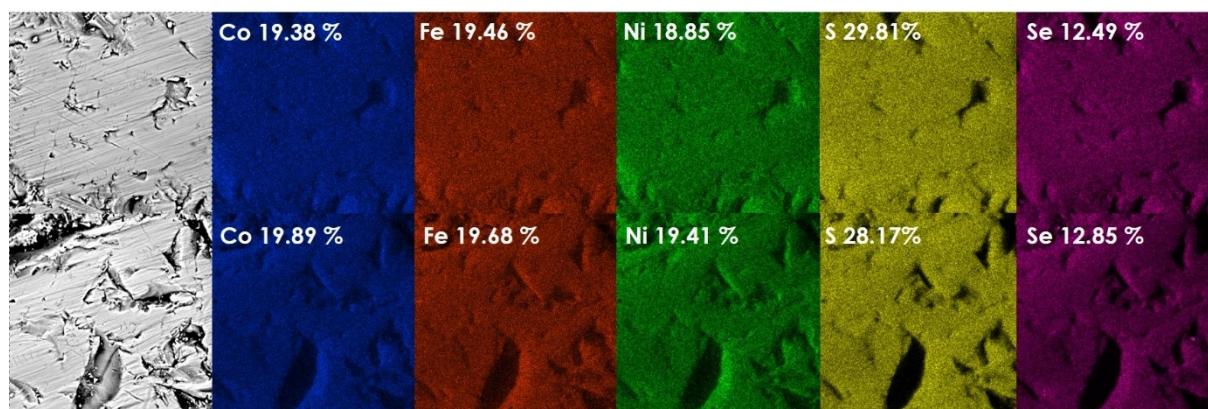
SI Fig.12 Chronoamperometric curves in 0.5 M H<sub>2</sub>SO<sub>4</sub>, recorded at constant overpotential 300 mV vs RHE.



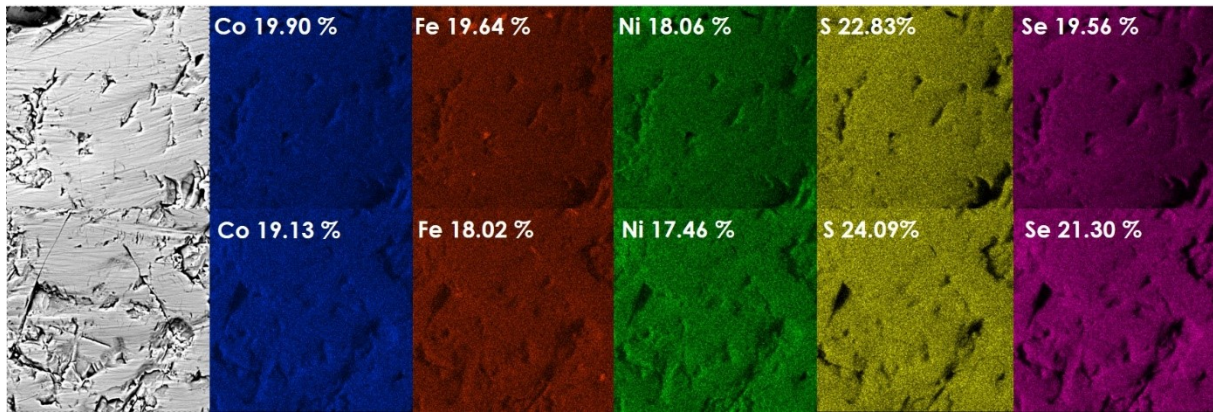
SI Fig.13 SEM micrographs together with EDS map analyses for  $\text{Co}_3\text{Fe}_3\text{Ni}_3\text{S}_8$  sample before (top) and after 2h electrolysis (bottom)



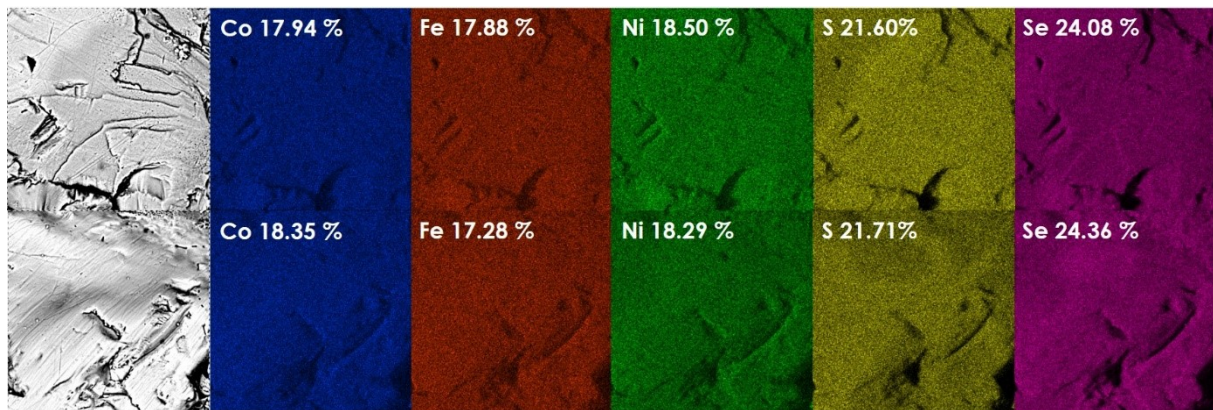
SI Fig.14 SEM micrographs together with EDS map analyses for  $\text{Co}_3\text{Fe}_3\text{Ni}_3\text{S}_7\text{Se}$  sample before (top) and after 2h electrolysis (bottom)



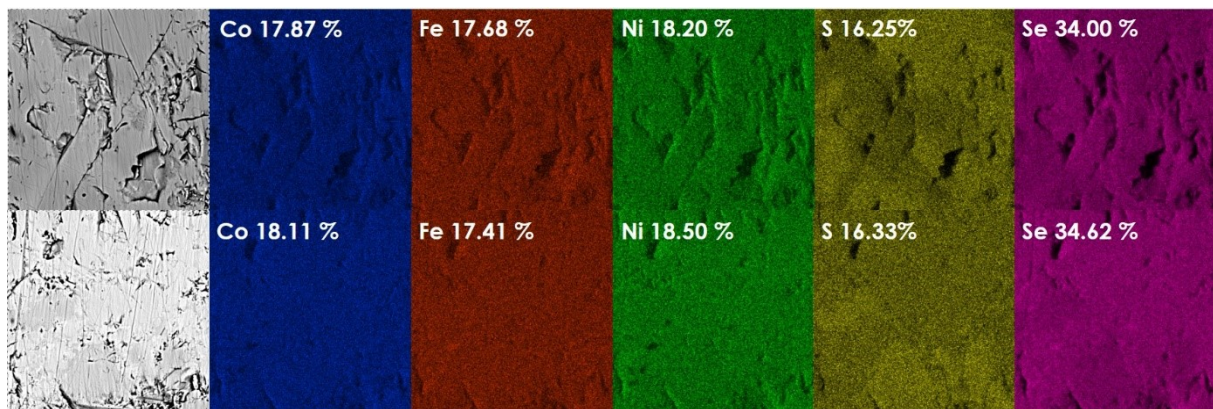
SI Fig.15 SEM micrographs together with EDS map analyses for  $\text{Co}_3\text{Fe}_3\text{Ni}_3\text{S}_6\text{Se}_2$  sample before (top) and after 2h electrolysis (bottom)



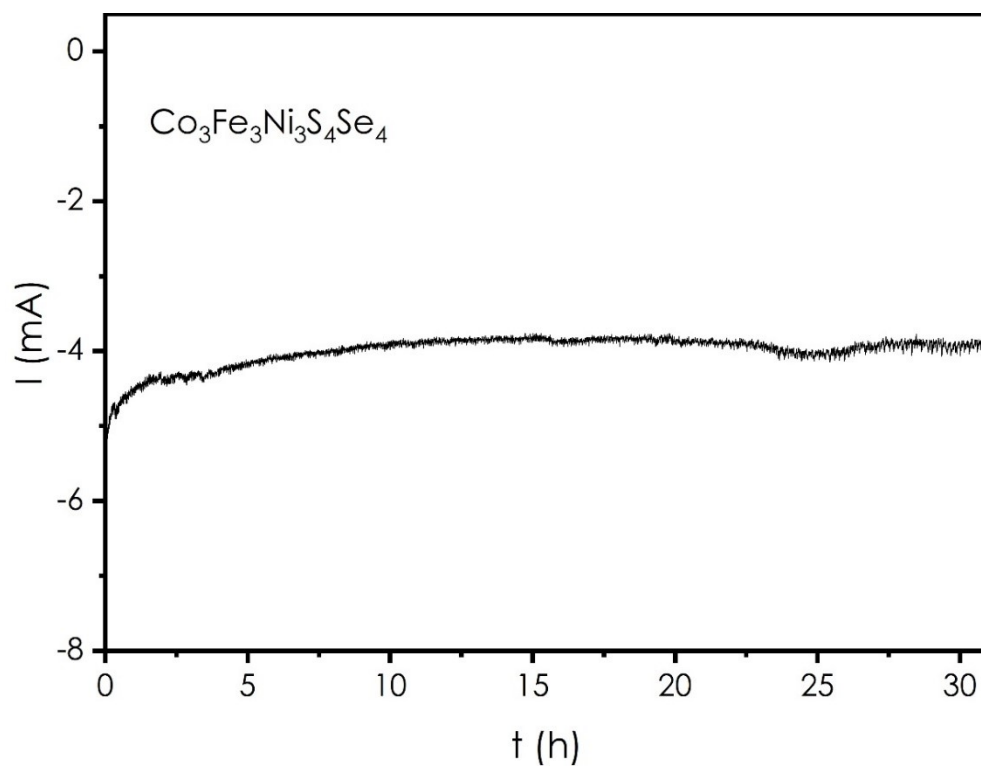
SI Fig.16 SEM micrographs together with EDS map analyses for  $\text{Co}_3\text{Fe}_3\text{Ni}_3\text{S}_5\text{Se}_3$  sample before (top) and after 2h electrolysis (bottom)



SI Fig.17 SEM micrographs together with EDS map analyses for  $\text{Co}_3\text{Fe}_3\text{Ni}_3\text{S}_4\text{Se}_4$  sample before (top) and after 2h electrolysis (bottom)



SI Fig.18 SEM micrographs together with EDS map analyses for  $\text{Co}_3\text{Fe}_3\text{Ni}_3\text{S}_3\text{Se}_5$  sample before (top) and after 2h electrolysis (bottom)



SI Fig.19 Chronoamperometric curve in 0.5 M  $\text{H}_2\text{SO}_4$  recorded at constant overpotential 300 mV vs RHE for best-performing material  $\text{Co}_3\text{Fe}_3\text{Ni}_3\text{S}_4\text{Se}_4$ .

SI Table 1 Density of the samples as a function of sintering temperature, selenium concentration and initial powder particle size (the densities values correspond directly to the samples that would be proceed in the next sections. Other series indicate very similar values).

Chemical composition	Sintering temperature [°C]	Density [g cm <sup>-3</sup> ]		Relative density [%]	
		Random particle size	Particle size 700–800 nm	Random particle size	Particle size 700–800 nm
Co <sub>3</sub> Fe <sub>3</sub> Ni <sub>3</sub> S <sub>8</sub>	400	4.380	4.784	85.547	93.438
Co <sub>3</sub> Fe <sub>3</sub> Ni <sub>3</sub> S <sub>7</sub> Se	400	4.207	5.063	79.079	95.169
Co <sub>3</sub> Fe <sub>3</sub> Ni <sub>3</sub> S <sub>6</sub> Se <sub>2</sub>	400	4.492	5.210	81.377	94.384
Co <sub>3</sub> Fe <sub>3</sub> Ni <sub>3</sub> S <sub>5</sub> Se <sub>3</sub>	400	4.567	5.421	79.843	94.773
Co <sub>3</sub> Fe <sub>3</sub> Ni <sub>3</sub> S <sub>4</sub> Se <sub>4</sub>	400	4.819	5.626	81.402	95.034
Co <sub>3</sub> Fe <sub>3</sub> Ni <sub>3</sub> S <sub>3</sub> Se <sub>5</sub>	400	5.116	5.702	83.595	93.170
Co <sub>3</sub> Fe <sub>3</sub> Ni <sub>3</sub> S <sub>8</sub>	400	4.380	4.784	85.547	93.438
Co <sub>3</sub> Fe <sub>3</sub> Ni <sub>3</sub> S <sub>8</sub>	450	4.792	4.888	93.594	95.468
Co <sub>3</sub> Fe <sub>3</sub> Ni <sub>3</sub> S <sub>8</sub>	500	4.983	4.969	97.324	97.053

SI Table 2 Basic electrocatalytic performance: overpotential vs RHE as a function of current density and calculated Tafel slopes of the sintered pentlandites with random particle sizes as a function of Se concentration.

Chemical composition (random particle size)	Overpotential at 120 mA cm <sup>-2</sup> [mV] vs RHE		Overpotential at 200 mA cm <sup>-2</sup> [mV] vs RHE		Tafel slope [mV dec <sup>-1</sup> ]	
	1 <sup>st</sup> cycle	After 2h	1 <sup>st</sup> cycle	After 2h	1 <sup>st</sup> cycle	After 2h
Co <sub>3</sub> Fe <sub>3</sub> Ni <sub>3</sub> S <sub>8</sub>	367	398	428	467	301	264
Co <sub>3</sub> Fe <sub>3</sub> Ni <sub>3</sub> S <sub>7</sub> Se	505	517	out of range	out of range	397	246
Co <sub>3</sub> Fe <sub>3</sub> Ni <sub>3</sub> S <sub>6</sub> Se <sub>2</sub>	518	534	out of range	out of range	360	343
Co <sub>3</sub> Fe <sub>3</sub> Ni <sub>3</sub> S <sub>5</sub> Se <sub>3</sub>	548	out of range	out of range	out of range	299	229
Co <sub>3</sub> Fe <sub>3</sub> Ni <sub>3</sub> S <sub>4</sub> Se <sub>4</sub>	338	329	384	375	209	204
Co <sub>3</sub> Fe <sub>3</sub> Ni <sub>3</sub> S <sub>3</sub> Se <sub>5</sub>	331	367	362	404	139	130

SI Table 3 Overpotentials at certain current densities for  $\text{Co}_3\text{Fe}_3\text{Ni}_3\text{S}_{8-x}\text{Se}_x$  (normalized series) solid electrodes versus chosen literature data

Sample	Overpotential [mV]			Reference
	at 10 mA cm <sup>-2</sup>	at 50 mA cm <sup>-2</sup>	at 100 mA cm <sup>-2</sup>	
$\text{Co}_3\text{Fe}_3\text{Ni}_3\text{S}_8$ (normalized to ECSA)	-	338	427	This work
$\text{Co}_3\text{Fe}_3\text{Ni}_3\text{S}_8$ (geom. area)	-	350	449	This work
$\text{Co}_3\text{Fe}_3\text{Ni}_3\text{S}_7\text{Se}$ (normalized to ECSA)	-	296	370	This work
$\text{Co}_3\text{Fe}_3\text{Ni}_3\text{S}_7\text{Se}$ (geom. area)	-	292	362	This work
$\text{Co}_3\text{Fe}_3\text{Ni}_3\text{S}_6\text{Se}_2$ (normalized to ECSA)	-	272	344	This work
$\text{Co}_3\text{Fe}_3\text{Ni}_3\text{S}_6\text{Se}_2$ (geom. area)	-	319	399	This work
$\text{Co}_3\text{Fe}_3\text{Ni}_3\text{S}_5\text{Se}_3$ (normalized to ECSA)	-	-	315	This work
$\text{Co}_3\text{Fe}_3\text{Ni}_3\text{S}_5\text{Se}_3$ (geom. area)	-	350	441	This work
$\text{Co}_3\text{Fe}_3\text{Ni}_3\text{S}_4\text{Se}_4$ (normalized to ECSA)	-	192	253	This work
$\text{Co}_3\text{Fe}_3\text{Ni}_3\text{S}_4\text{Se}_4$ (geom. area)	-	241	302	This work
$\text{Co}_3\text{Fe}_3\text{Ni}_3\text{S}_3\text{Se}_5$ (normalized to ECSA)	-	226	283	This work
$\text{Co}_3\text{Fe}_3\text{Ni}_3\text{S}_3\text{Se}_5$ (geom. area)	-	326	394	This work
$\text{Fe}_{4.5}\text{Ni}_{4.5}\text{S}_8$ (normalized to ECSA)	292	332	355	This work
$\text{Fe}_{4.5}\text{Ni}_{4.5}\text{S}_8$	319	385	-	28,58
$\text{Co}_3\text{Fe}_3\text{Ni}_3\text{S}_8$	285	376	-	58
$\text{Fe}_{4.5}\text{Ni}_{4.5}\text{S}_4\text{Se}_4$	~320	~395	-	30
$\text{Ni}_3\text{Se}_4/\text{CC}$	~100	~240	~350	40
$\text{Ni}_{1.86}\text{Co}_{1.05}\text{Fe}_{0.09}\text{Se}_4/\text{CC}$	~87	~200	~300	40
$\text{Ni}_3\text{Se}_4@\text{MoSe}_2$	242	~300	-	59

SI Table 4 HER performance as a function of density, electrochemical active surface area and chemical composition.

Chemical composition	series	Overpotential at 120 mA cm <sup>-2</sup> [mV]	Tafel slope [mV dec <sup>-1</sup> ]	ECSA [mm <sup>2</sup> ]	Density [%]
$\text{Co}_3\text{Fe}_3\text{Ni}_3\text{S}_8$	IHP random particle size	367	301	2.0	85,5
$\text{Co}_3\text{Fe}_3\text{Ni}_3\text{S}_7\text{Se}$		505	397	9.7	79
$\text{Co}_3\text{Fe}_3\text{Ni}_3\text{S}_6\text{Se}_2$		518	360	5.5	81,4
$\text{Co}_3\text{Fe}_3\text{Ni}_3\text{S}_5\text{Se}_3$		548	299	7.4	79,8
$\text{Co}_3\text{Fe}_3\text{Ni}_3\text{S}_4\text{Se}_4$		338	209	1.0	81,4
$\text{Co}_3\text{Fe}_3\text{Ni}_3\text{S}_3\text{Se}_5$		331	139	0.8	83,6
$\text{Co}_3\text{Fe}_3\text{Ni}_3\text{S}_8$	IHP normalized particle size	460	217	4.4	93,4
$\text{Co}_3\text{Fe}_3\text{Ni}_3\text{S}_7\text{Se}$		398	154	13.7	95,2
$\text{Co}_3\text{Fe}_3\text{Ni}_3\text{S}_6\text{Se}_2$		363	230	3.0	94,4
$\text{Co}_3\text{Fe}_3\text{Ni}_3\text{S}_5\text{Se}_3$		333	234	1.7	94,8
$\text{Co}_3\text{Fe}_3\text{Ni}_3\text{S}_4\text{Se}_4$		264	213	2.5	95
$\text{Co}_3\text{Fe}_3\text{Ni}_3\text{S}_3\text{Se}_5$		296	184	1.3	93,2